Chapter 5

Deformation of Glass-Forming Metallic Liquids: Configurational Changes and Their Relation to Elastic Softening

Amorphous metal, Elastic properties, Shear transformation zone, Ultrasonic measurement, Compression test, Glass, Enthalpy relaxation

5.1 Abstract

The change in the configurational enthalpy of metallic-glass-forming liquids induced by mechanical deformation and its effect on elastic softening is assessed. The acoustically measured shear modulus is found to decrease with increasing configurational enthalpy by a dependence similar to one obtained by softening via thermal annealing. This establishes that elastic softening is governed by a unique functional relationship between shear modulus and configurational enthalpy.

5.2 Introduction

There have been many theories put forward to explain the deformation processes observed in metallic glasses. One theory involves the free volume of the material associated with different configurational states [1-6]. In this theory a dilatation of the material's free volume is directly linked to changes in the viscosity of the material. This basic concept has been applied in many different ways to explain the flow processes observed in experiments. Efforts to measure the free volume concentration versus the viscosity of the material have been attempted. The boundary between homogenous and inhomogeneous deformation has also been described using free volume. Furthermore, shear localization has been described as being a catastrophic production of free volume in the region of the formed shear band.

Argon put forward two separate mechanisms for the deformation of metallic glasses [7-9]. He proposed that in the low temperature limit the energetically favored transformation configuration is in the shape of a thin disk containing the shear transformation direction in its plane, and in that limit this gives a dislocation loop. This was the description for the shear localization regime. For the homogenous deformation regimes Argon envisioned local clusters of atoms that were mechanically polarized due to an applied stress field. Those shear transformation zones (STZs) were envisioned to cooperatively flow together resulting in permanent deformation. The STZs that did not cooperatively flow were thought to be responsible for the anelastic properties observed in metallic glasses.

Another theory that attempts to explain the irreversible structural relaxation and homogeneous plastic flow seen in metallic glasses is the Directional Structural

Relaxation model (DSR). In this model homogeneous flow is viewed simply as a result of structural relaxation oriented in the direction of an external stress field [10]. Further DSR models have been proposed in which shear localization and homogeneous flow are dictated by a potential energy landscape. Therefore, it is a stochastic process that determines when and where a DSR event would occur [11].

In the recent work of Johnson and co-workers [12-15], a link between elastic softening and configurational changes in metallic-glass-forming liquids has been proposed. The steepness of the viscosity dependence on temperature in the vicinity of the glass transition, i.e., the liquid fragility, has been known to be associated with the stored configurational enthalpy since the early work of Angell [16-18]. Furthermore, the effect of strain rate on viscosity induced by mechanical deformation has also been linked to changes in configurational enthalpy [6]. However, attributing the deformationally induced softening of liquids to a unique functional relation between shear modulus and stored configurational enthalpy is a concept that has just recently been brought to attention [14]. This concept essentially suggests that conversion of mechanical work into stored configurational enthalpy induces softening via a dependence of shear modulus on configurational enthalpy. The thermodynamic state variable controlling flow in this concept is identified to be the isoconfigurational shear modulus. Experimental validation of earlier concepts based on the "free volume" hypothesis [1] has not been possible, mainly due to the lack of a fundamental thermodynamic definition of "free volume." In contrast, the isoconfigurational shear modulus is a thermodynamically well-defined and experimentally accessible property, rendering this concept experimentally verifiable. In the present study, the change in configurational enthalpy induced by mechanical work

and its effect on the softening of metallic-glass-forming liquids is evaluated by means of compressive experiments, ultrasonic measurements, and enthalpy recovery tests.

5.3 Experimental

For the loading experiments we used cast cylindrical specimens of $Pt_{57.2}Ni_{5.3}Cu_{14.7}P_{22.5}$ [19, 20] and $Pd_{43}Ni_{10}Cu_{27}P_{20}$ [21, 22], which we deformed isothermally at constant strain rates. The loading setup described in Ref. [23] was utilized. Deformation was performed for a period of time sufficient to allow a steady flow stress state in the non-Newtonian regime to be attained. Upon unloading, the specimens were quenched as rapidly as possible in order to capture the configurational state associated with that flow stress.

We assessed the elastic softening induced by mechanical deformation by evaluating the isoconfigurational shear modulus at the high-frequency "solid-like" limit, *G*. We evaluated *G* of the quenched unloaded specimens ultrasonically [24], and we subsequently extrapolated the room-temperature measurements to estimate *G* at the temperatures of the flow experiments using linear Debye-Grüneisen coefficients to account for the thermal expansion effect on the shear modulus of the glass. Shear wave speeds were measured using the pulse-echo overlap set-up described in Ref. [13]. Densities were measured by the Archimedes method, as given in the American Society for Testing and Materials standard C693-93.

Additional experiments were done to evaluate the elastic softening of the materials with respect to temperature. We relaxed samples at temperatures ranging from 473 K to 503 K for $Pt_{57.2}Ni_{5.3}Cu_{14.7}P_{22.5}$, and 548 K to 573 K for $Pd_{43}Ni_{10}Cu_{27}P_{20}$. Again the specimens were quenched as rapidly as possible to retain the configurational state associated with each temperature. The elastic properties were evaluated at each temperature and it was shown that the relaxation process was completely reversible in

agreement with Ref. [13], thus indicating that the measured properties relate to equilibrium states.

We assessed the configurational changes induced by mechanical deformation by evaluating the configurational enthalpy stored in the deformed specimens, Δh. Reference samples were created by relaxing $Pt_{57.2}Ni_{5.3}Cu_{14.7}P_{22.5}$ and $Pd_{43}Ni_{10}Cu_{27}P_{20}$ specimens at 473 K and 548 K, respectively. The reference temperatures are the same as those in the continuous strain-rate experiments. The specimens were allowed to relax at those temperatures for a total of 50 hr to ensure that the glass obtained an equilibrium configurational state. We take Δh to be the change in the recovered enthalpy in reference to that relaxed undeformed state, as measured using Differential Scanning Calorimetry (DSC) [25]. A Netzch DSC 404C was employed at a scan rate of 10 K/min for the measurements.

The recovered enthalpy corresponds to an endothermic process in which the specimens absorb energy to bring the glass back into an equilibrium energy state at the glass transition temperature. This endothermic process occurs because the specimens have been relaxed to an energy state below the equilibrium energy state at the glass transition temperature. Therefore, when the specimens reach the glass transition temperature, i.e., a laboratory time scale, an increase in the energy of the specimens is observed. The change in the total amount of energy absorbed shown in the DSC scans for the different strain rates is due to the amount of energy imparted to the specimens during deformation. The specimens that were deformed at higher strain rates absorbed more energy. Hence, the endothermic peaks shown in the DSC curves become smaller as

the strain rate is increased. The dependence of G on Δh is assessed by plotting the changes in shear modulus against the respective changes in the stored enthalpy.

For a more detailed account of specimen preparation, mechanical testing, and the property evaluation techniques used please see the experimental section in Chapter 2.3. For the preparation of $Pt_{57.2}Ni_{5.3}Cu_{14.7}P_{22.5}$ please see Chapter 3.3.

5.4 Discussion

First, we attempt to investigate the effect of isothermal constant strain rate deformation on *G*. We deformed two $Pd_{43}Ni_{10}Cu_{27}P_{20}$ specimens, both at a temperature of 548 K and a strain rate of 10^{-4} s^{-1}. One of the specimens was at the as-cast non-equilibrium state, while the other had been previously relaxed by annealing at 548 K for 50 hr. The stress-strain responses are shown in Fig. 5.1.

Both specimens are shown to undergo a transient relaxation response (characterized by a stress overshoot) towards a steady non-equilibrium flow-stress state. As a consequence of having different initial structural states the transient stress overshoot during relaxation is dramatically different for the two specimens. However, the steady flow stress states are very similar. It is therefore demonstrated that the steady flow stress state at a given temperature and strain rate is unique, independent of the initial structural state. The relaxation process exemplified by the transient stress-strain response in fact constitutes a general relaxation process for all material properties, including configurational energy as well as shear modulus. The measured shear modulus for each specimen before and after deformation is presented in Fig. 5.2. As expected, prior to deformation the shear modulus of the relaxed specimen is considerably higher than that of the as-cast specimen, which is a consequence of the relaxed specimen being at a lower-energy equilibrium state. After deformation, the shear modulus of the relaxed specimen is shown to undergo a relaxation process towards a lower steady value, while the shear modulus of the as-cast specimen is shown to relax to a higher steady value. The post-deformation shear moduli are shown to be nearly identical. We have therefore

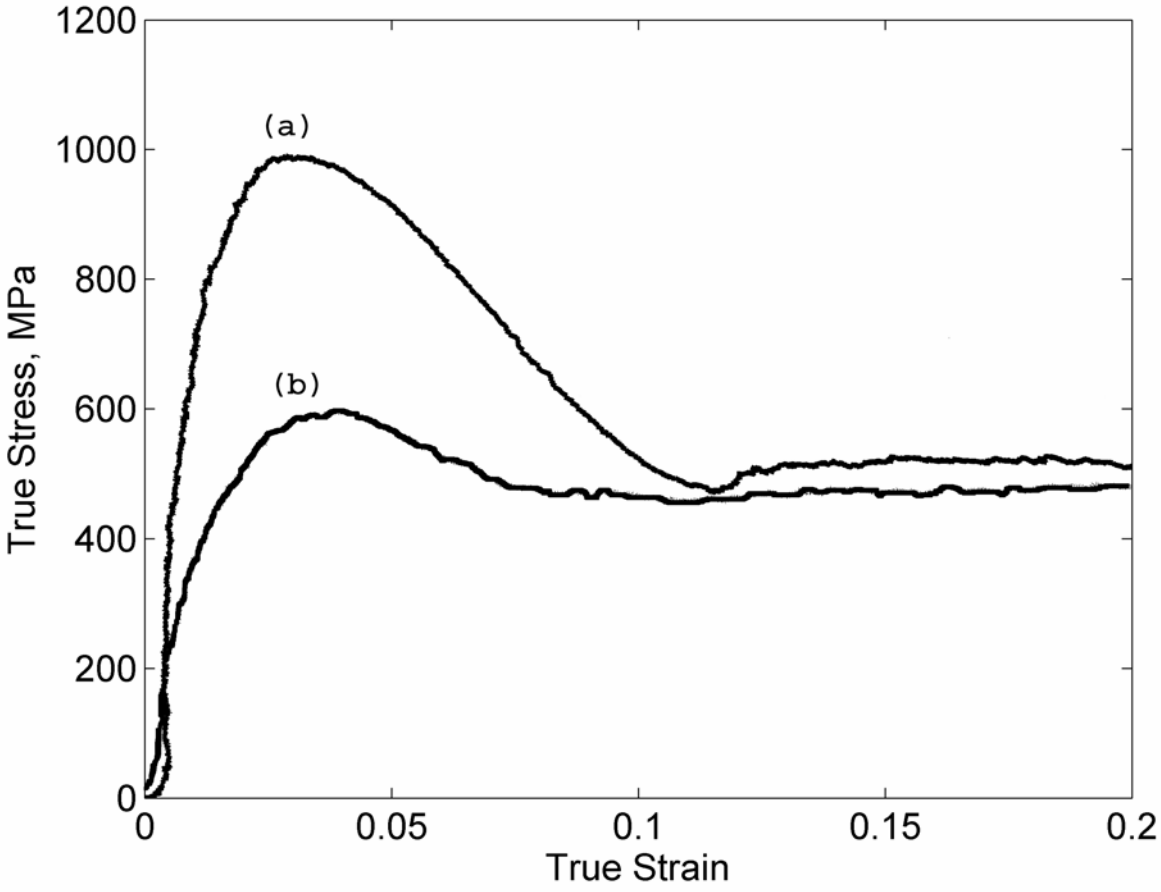

Figure 5.1. True stress-strain curves for two $Pd_{43}Ni_{10}Cu_{27}P_{20}$ specimens deformed at 548 K and a strain rate of $1.0x10^{-4}$ s^{-1}: **(a)** specimen was relaxed at 548 K prior to deformation, and **(b)** specimen was in the as-cast state.

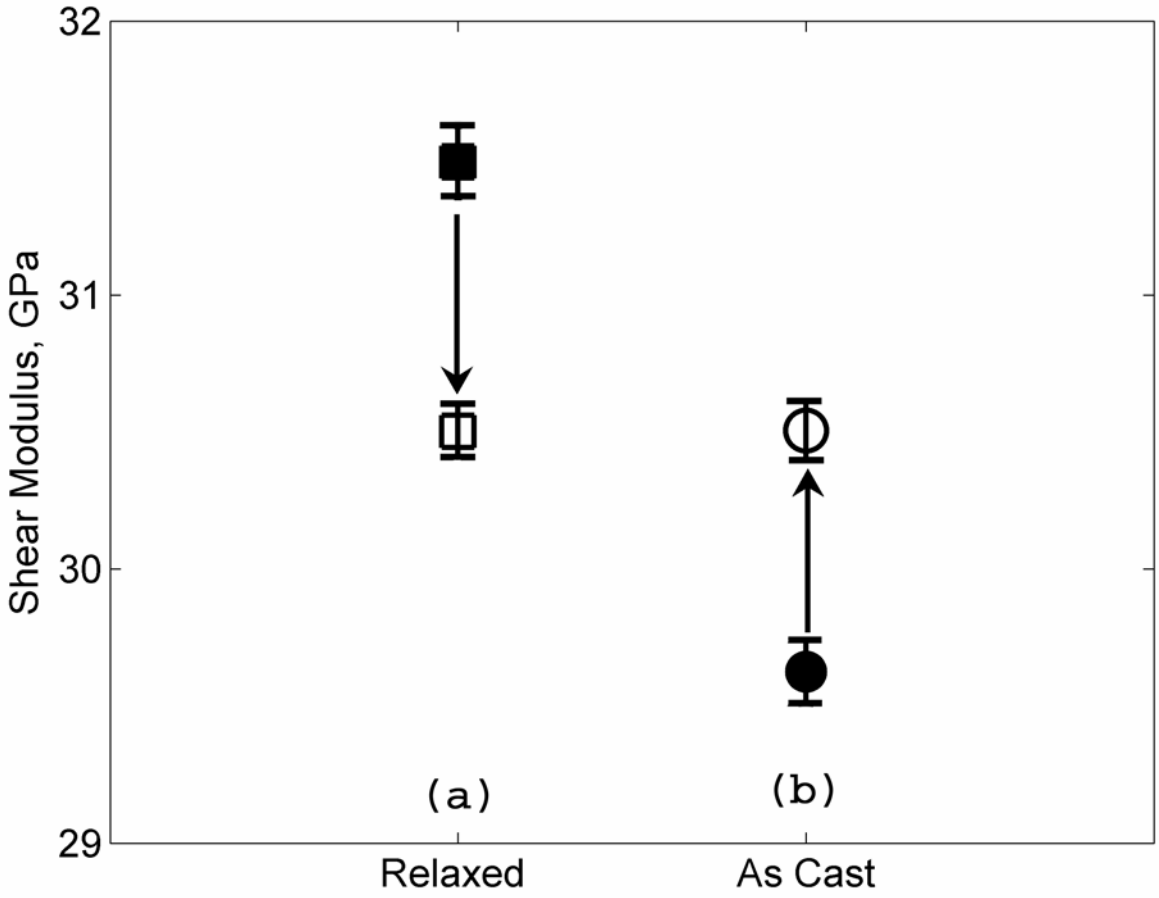

Figure 5.2. (a) shear modulus of the relaxed specimen before (■) and after deformation (□), **(b)** shear modulus of the as-cast specimen before (●) and after deformation (○)

demonstrated that the steady non-equilibrium state attained under a given flow stress is unique, and is associated with a corresponding steady-state shear modulus, regardless of the initial state of the glass.

Since steady state is independent of the initial structural state, we have chosen to proceed with our analysis using as-cast specimens. The as-cast specimens are at a higher initial energy state than the relaxed specimens. Consequently, the specimen's transient response to an applied strain rate results in a lower peak stress. This response is due to the specimen being in a "softer" state, since the glass has been kinetically frozen at a higher temperature than in the relaxed specimens. Since the peak stress is lower for the as-cast specimens, the onset of shear localization is delayed to higher strain rates. This allowed us to observe the material properties over a greater range of strain rates for homogeneous flow. In Fig. 5.3 we present the stress strain curves for $Pt_{57.2}Ni_{5.3}Cu_{14.7}P_{22.5}$ and $Pd_{43}Ni_{10}Cu_{27}P_{20}$.

As noted in Fig. 5.1 and 5.3, the transient relaxation process is completed at a strain of 10-11% in all tests. This strain limit is observed in essentially all mechanical tests performed in metallic-glass-forming liquids. In Johnson et. al. [12] a theory based on Shear Transformation Zones (STZs) is put forward. It was assumed that there was a periodic Frenkel Potential that defined the energy landscape for the basic unit of deformation, the STZs. That Frenkel Potential was given in the form $\phi(\gamma) = \phi_0 \sin^2(\pi\gamma / 4\gamma_C)$. When a stress field is applied to the energy landscape it tilts the barriers in the manner of $h(\gamma) = \phi(\gamma) - \tau\gamma$, where $h(\gamma)$ is the "free enthalpy" density of the stressed STZ. The effect of a stress field on the potential energy landscape is illustrated in Fig. 5.4. As can be seen, the distance between minima in the energy

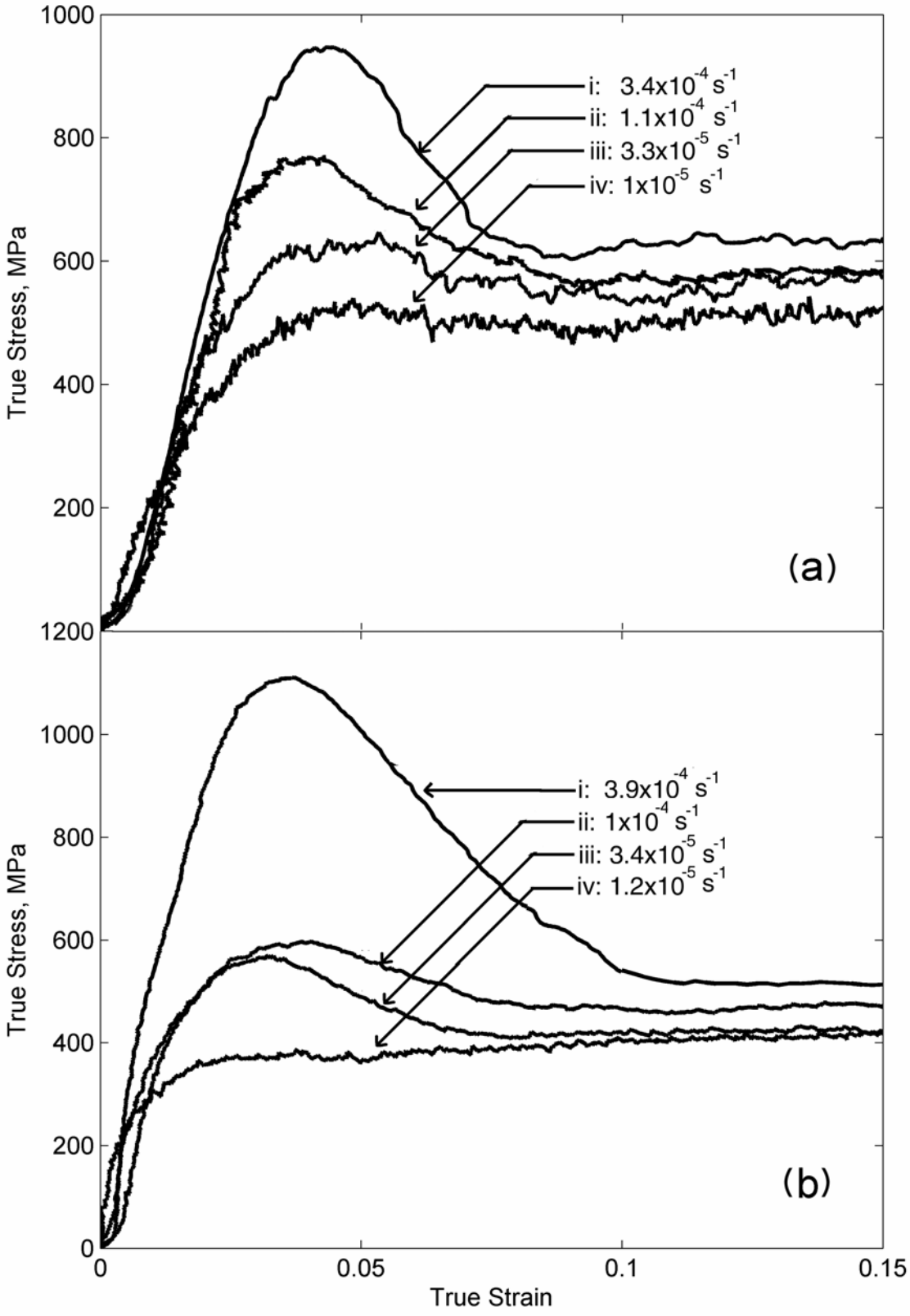

Figure 5.3. True stress-strain diagrams for **(a)** $Pt_{57.2}Ni_{5.3}Cu_{14.7}P_{22.5}$ at 473 K and **(b)** $Pd_{43}Ni_{10}Cu_{27}P_{20}$ at 548 K at the indicated strain rates

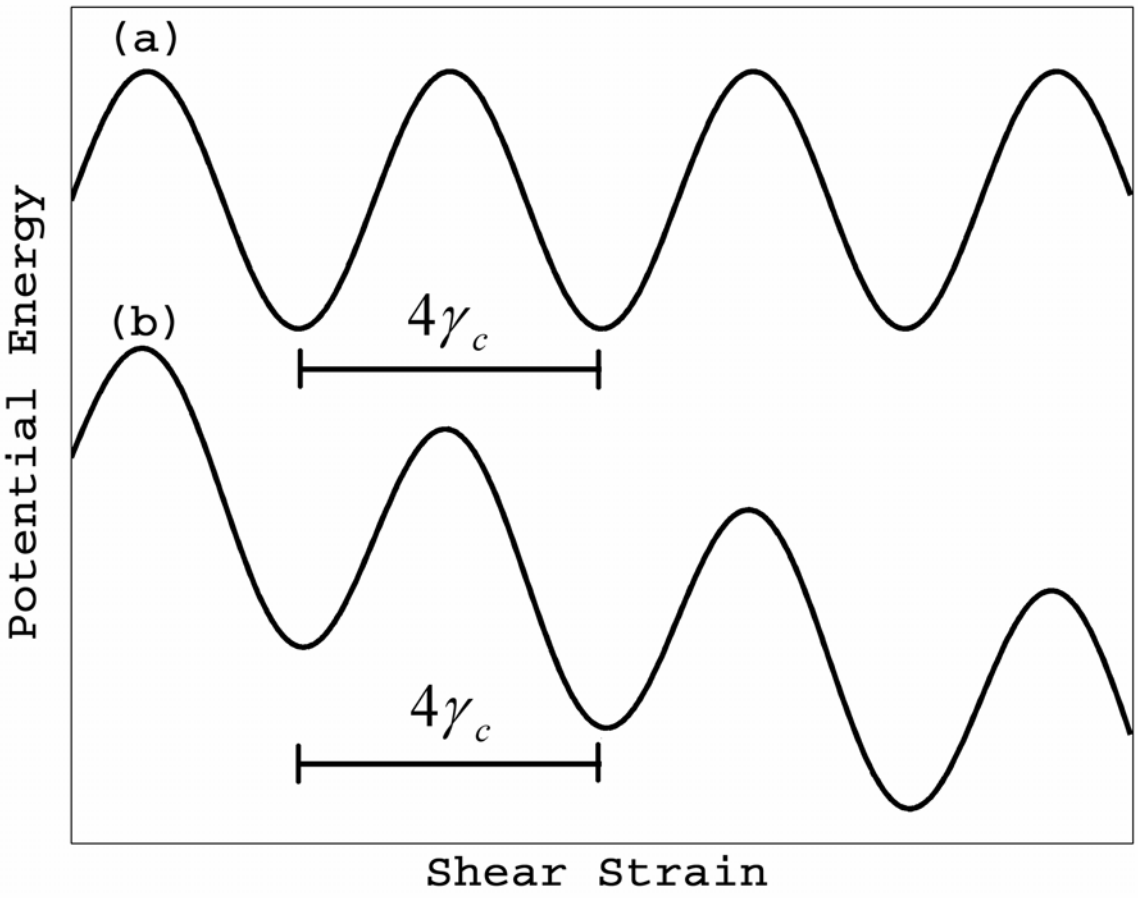

Figure 5.4. (a) Frenkel Potential Energy Landscape with a strain of $4\gamma_c$ between minima, **(b)** A Frenkel Potential Energy Landscape that has been biased by a stress. The strain between minima is still $4\gamma_c$.

landscape remains constant even under an applied stress field. The configurational strain (shear strain between saddles in configurational space) is found to be $\gamma_c = 0.036$ for all metallic-glass-forming systems [12]. A single barrier crossing event would therefore require a shear strain of $4\gamma_c = 4\times0.036$, which is equivalent to a uniaxial strain of ~ 0.105 (for a Poisson's ratio of ~ 0.37). This strain is equivalent to the strain at which the specimens reach steady-state deformation. Furthermore, since the specimen has reached steady state at the strain corresponding to the strain of a single barrier-crossing event it implies that, on average, each STZ has undergone one complete barrier-crossing event when the specimen reaches steady state deformation. Once steady state is attained at this critical strain, configurational changes are no longer registered in the material and essentially all of the mechanical work is dissipated as heat.

In Fig. 5.5 we present the DSC traces for the deformed specimens as well as the undeformed relaxed specimens. In Table 5.1 we present the configurational enthalpies stored at each steady state, as evaluated from the DSC traces.

	Δh at (i) [MJ/m^3]	Δh at (ii) [MJ/m^3]	Δh at (iii) [MJ/m^3]	Δh at (iv) [MJ/m^3]
$Pt_{57.2}Ni_{5.3}Cu_{14.7}P_{22.5}$	74.2	66.5	52.8	45.7
$Pd_{43}Ni_{10}Cu_{27}P_{20}$	90.2	73.9	60.5	46.2

Table 5.1. Changes in configurational enthalpy for each steady flow state with respect to a relaxed, undeformed reference state assessed from enthalpy recovery tests. States (i) through (iv) correspond to the strain rates indicated in Fig. 5.3 and 5.5.

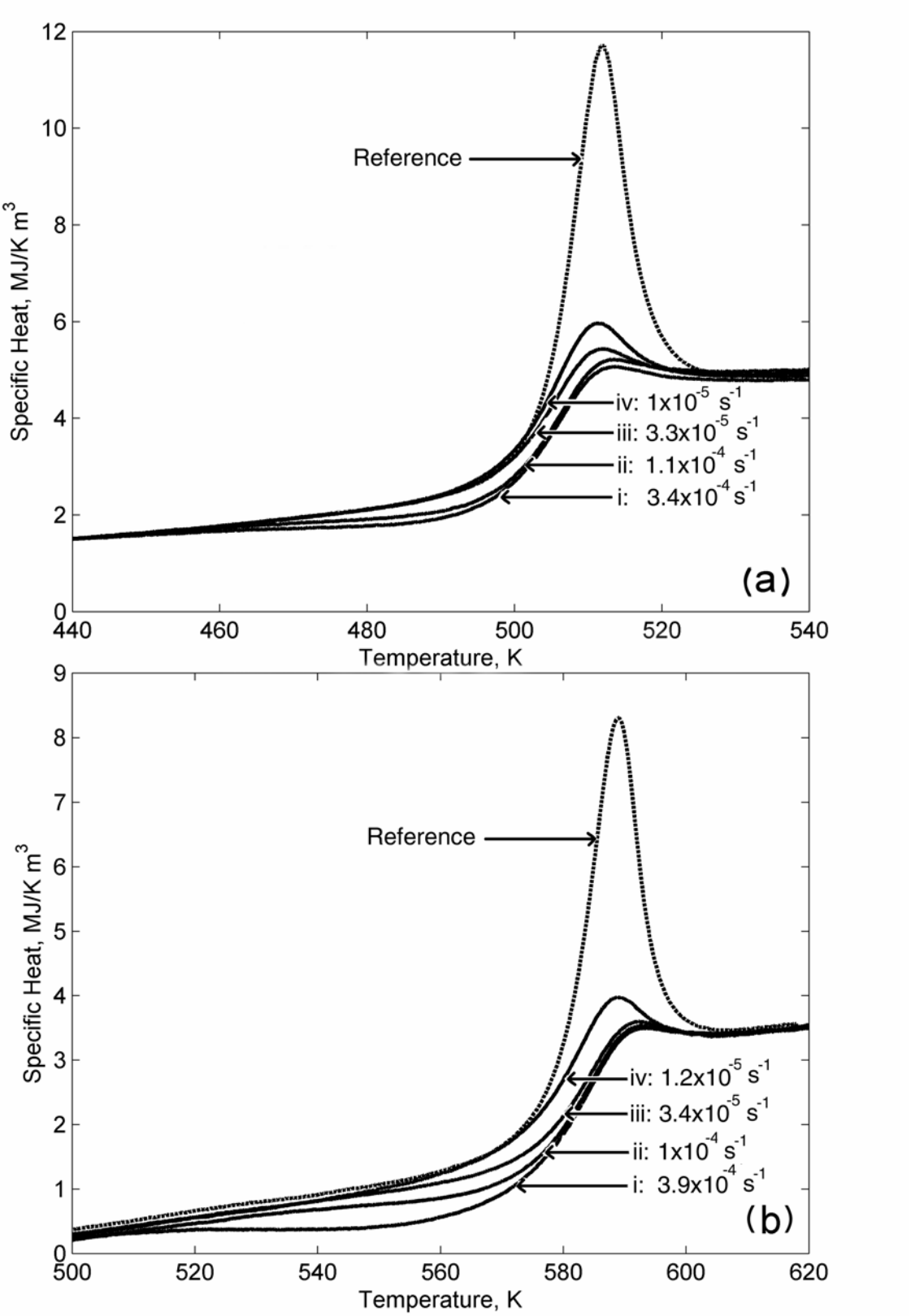

Figure 5.5. DSC traces obtained from the quenched unloaded specimens for **(a)** $Pt_{57.2}Ni_{5.3}Cu_{14.7}P_{22.5}$ and **(b)** $Pd_{43}Ni_{10}Cu_{27}P_{20}$. The loading strain rates are indicated.

In Table 5.2 we present the shear moduli of the deformed specimens associated with the respective steady flow states, as measured acoustically and corrected for the Debye-Grüneisen effect. We utilized measured linear Debye-Grüneisen coefficients of 13 MPa/K for $Pt_{57.2}Ni_{5.3}Cu_{14.7}P_{22.5}$ [26] and 15 MPa/K for $Pd_{43}Ni_{10}Cu_{27}P_{20}$ [27].

	G at (i) [GPa]	*G* at (ii) [GPa]	*G* at (iii) [GPa]	*G* at (iv) [GPa]
$Pt_{57.2}Ni_{5.3}Cu_{14.7}P_{22.5}$	29.84±0.24	30.02±0.31	30.43±0.40	30.74±0.32
$Pd_{43}Ni_{10}Cu_{27}P_{20}$	30.20±0.09	30.50±0.11	30.94±0.09	31.16±0.12

Table 5.2. Isoconfigurational shear modulus for each steady flow state, as measured acoustically on each quenched unloaded specimen and corrected for the Debye-Grüneisen effect. States (i) through (iv) correspond to the strain rates indicated in Fig. 5.3 and 5.5. The larger errors in the measurements of $Pt_{57.2}Ni_{5.3}Cu_{14.7}P_{22.5}$ specimens are due to the use of smaller mechanical specimens, which produced a higher uncertainty in the measured density.

In order to evaluate the thermodynamic dependence of G on Δh, we plot their respective values in Fig. 5.6. As evidenced from this plot, G decreases with increasing Δh in an approximately linear fashion. This dependence of G on Δh is also supported by recent molecular dynamics simulations in which G was found to decrease linearly with increasing energy [15]. This finding supports that the elastic softening induced by mechanical deformation is essentially governed by the dependence of shear modulus on configurational enthalpy.

We argue that the dependence of G on Δh obtained here by mechanically deforming the liquid is a unique functional relation. We can validate this argument by comparing this dependence against one obtained via a different softening path. One such path is realized by inducing softening of the liquid by annealing at incrementally higher temperatures, as performed in Ref. [13]. The shear moduli for $Pt_{57.2}Ni_{5.3}Cu_{14.7}P_{22.5}$ and $Pd_{43}Ni_{10}Cu_{27}P_{20}$ specimens were measured after annealing treatments at temperatures

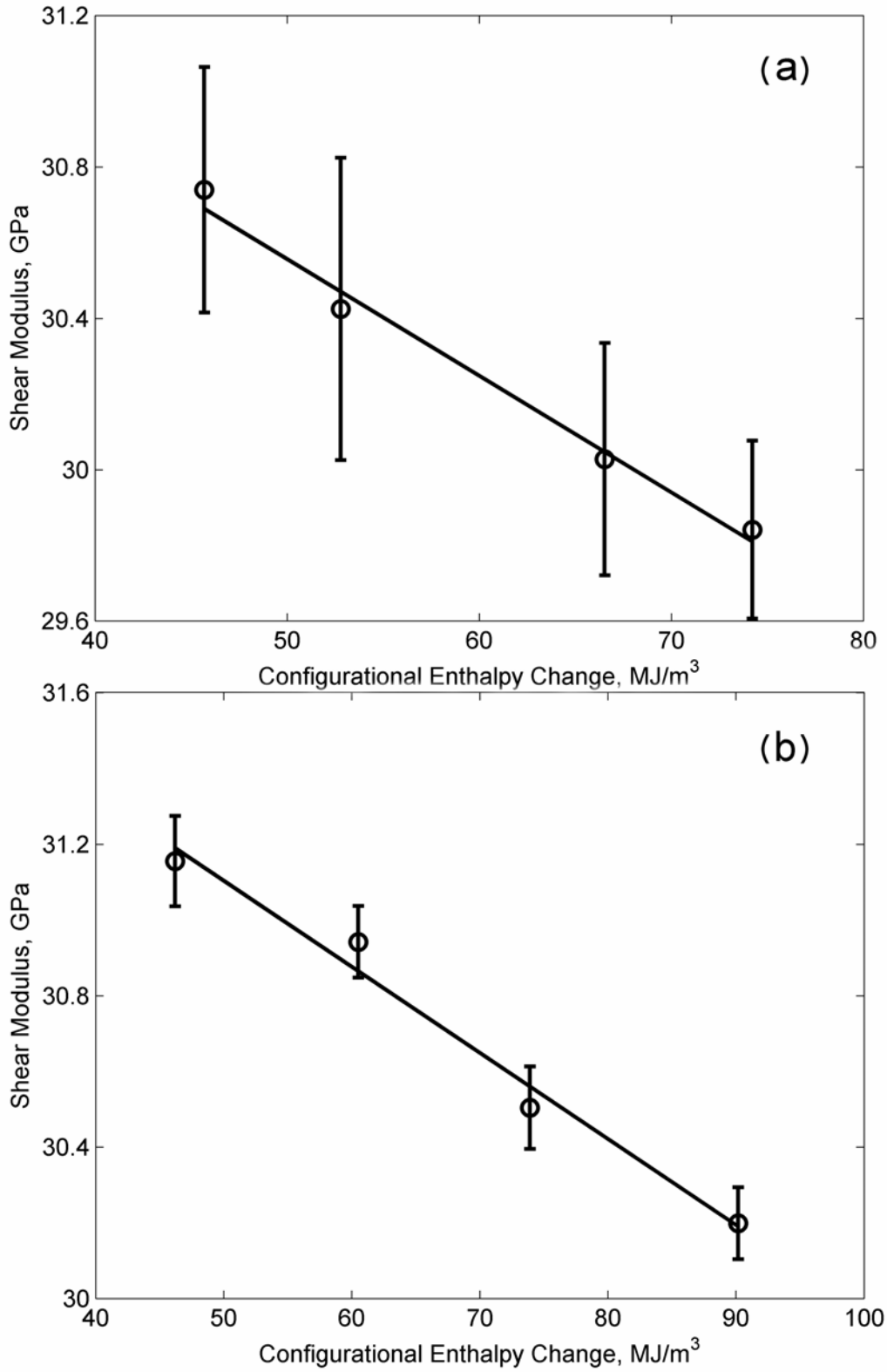

Figure 5.6. Isoconfigurational shear modulus vs. configuration enthalpy change for each steady flow state for **(a)** $Pt_{57.2}Ni_{5.3}Cu_{14.7}P_{22.5}$ and **(b)** $Pd_{43}Ni_{10}Cu_{27}P_{20}$. Dotted lines are linear regressions to the data.

ranging from 472 K to 503 K and 548 K to 573 K, respectively. The shear modulus is plotted against the relaxation temperature in Fig.7. The measured elastic properties were found to be completely reversible from one temperature to another, and therefore it may be assumed that the measured shear moduli correspond to unique equilibrium states.

Linearly fitting the data found in Fig. 5.7, we find $dG/dT \approx -80$ MPa/K for $Pt_{57.2}Ni_{5.3}Cu_{14.7}P_{22.5}$ and ≈ -56.5 MPa/K for $Pd_{43}Ni_{10}Cu_{27}P_{20}$. The change in specific heat, $d\Delta h/dT$, was evaluated from the DSC scans performed in the present study. The quantity for $d\Delta h/dT$ is taken as the change in heat capacity at the glass transition temperature.

The measured values for the change in specific heat for each alloy are $d\Delta h/dT =$ 2.56 MJ/m^{3}K for $Pt_{57.2}Ni_{5.3}Cu_{14.7}P_{22.5,}$ and 2.5 MJ/m^{3}K for $Pd_{43}Ni_{10}Cu27P_{20.}$ We now have values for both dG/dT and $d\Delta h/dT$ for each alloy. For the thermal annealing experiments the changes in shear modulus with respect to the changes in configurational enthalpy, $dG/d\Delta h = (dG/dT)/(d\Delta h/dT)$, can be calculated to be ≈ -31.3 for $Pt_{57.2}Ni_{5.3}Cu_{14.7}P_{22.5}$ and ≈ -22.6 for $Pd_{43}Ni_{10}Cu_{27}P_{20}$. For the mechanical deformation experiments performed in the present study $dG/d\Delta h$ can be calculated from Fig. 5.5 as ≈ -31.0 for $Pt_{57.2}Ni_{5.3}Cu_{14.7}P_{22.5}$ and ≈ -22.7 for $Pd_{43}Ni_{10}Cu_{27}P_{20}$.

The comparison between the thermal relaxation experiments and the mechanical deformations is shown in Fig. 5.8. An initial enthalpy, Δh, was assumed for the thermal relaxation experiments. Then using the values obtained for G(T) and $d\Delta h/dT$ a plot of G versus Δh is constructed. Again there is good agreement in the behavior of G with respect to Δh between the two experimental data sets for each alloy. We have therefore shown that for each alloy system, $dG/d\Delta h$ obtained from thermally annealing the liquid is approximately equivalent to $dG/d\Delta h$ obtained from mechanically deforming the liquid.

Hence, we can conclude that the dependence of G on Δh is a unique functional relation.

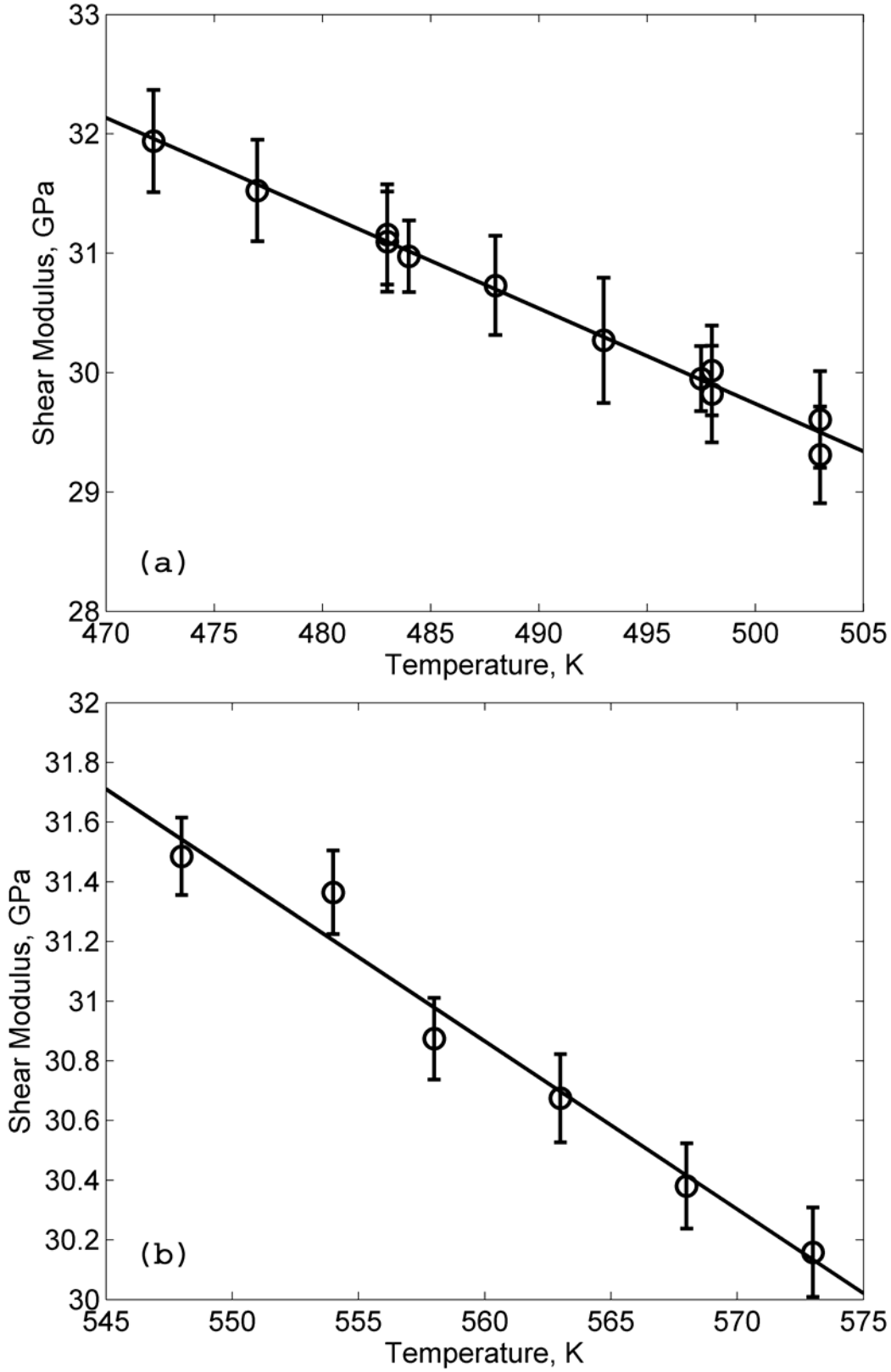

Figure 5.7. Isoconfigurational shear modulus versus annealing temperature for **(a)** $Pt_{57.2}Ni_{5.3}Cu_{14.7}P_{22.5}$ and **(b)** $Pd_{43}Ni_{10}Cu_{27}P_{20}$

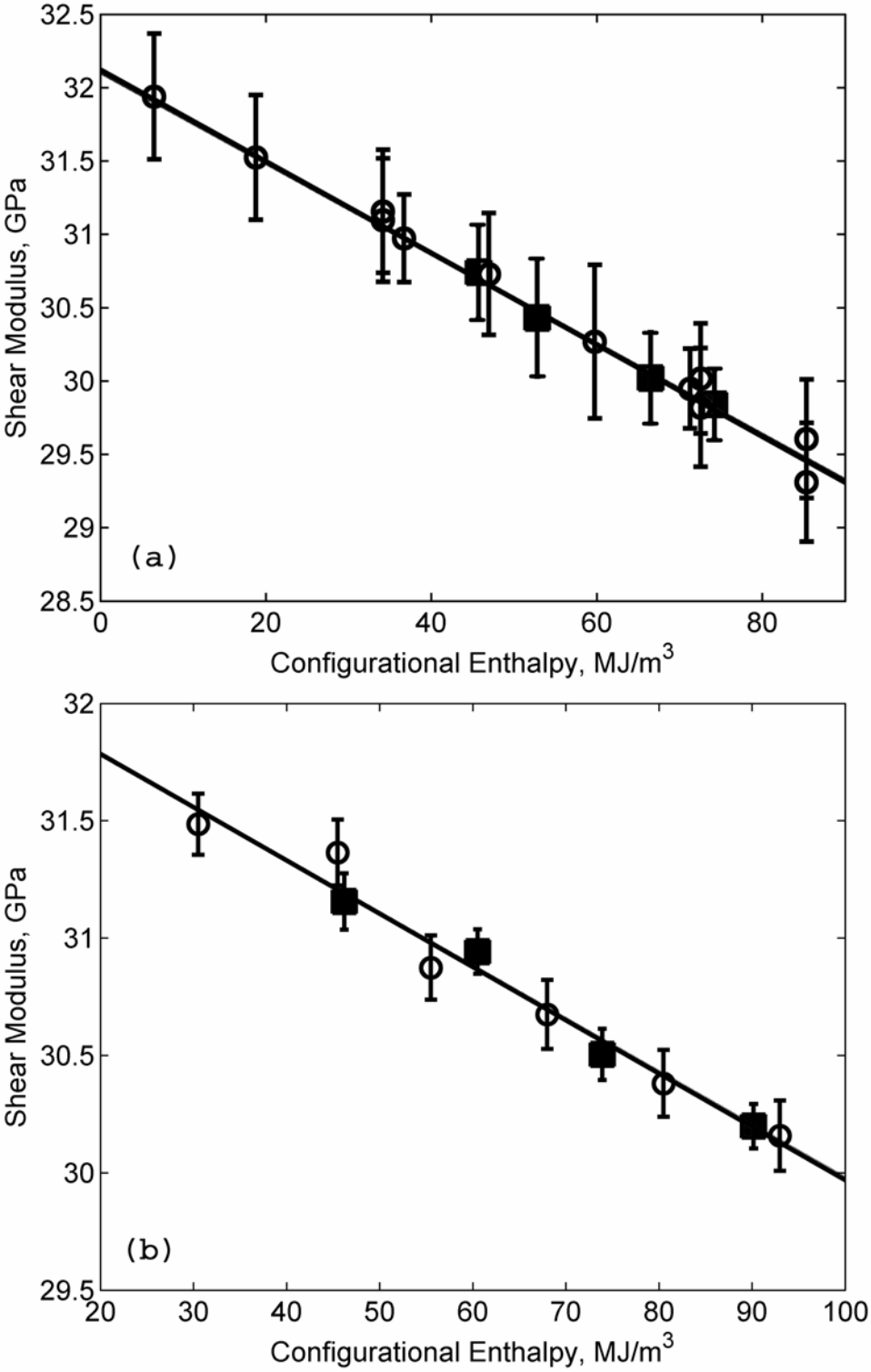

Figure 5.8. Isoconfigurational shear modulus versus configurational enthalpy is plotted for **(a)** $Pt_{57.2}Ni_{5.3}Cu_{14.7}P_{22.5}$ and **(b)** $Pd_{43}Ni_{10}Cu27P_{20}$ with (■) data obtained from the mechanical deformation experiments presented in Fig. 5.6 and (○) data converted from the thermal annealing experiments presented in Fig. 5.7. The linear regressions to the mechanical and thermal data sets are indistinguishable on this plot.

5.5 Conclusion

In conclusion, we evaluated the changes in the configurational enthalpy of metallic-glass-forming liquids induced by mechanical deformation, as well as their thermal relaxation, and assessed their effect on elastic softening. Subsequently, we evaluated the isoconfigurational shear modulus with respect to the stored configurational enthalpy of each specimen. We found that the isoconfigurational shear modulus decreases with increasing configurational enthalpy in an approximately linear trend for the deformation experiments. This trend is in agreement with recent molecular dynamics simulations. By recognizing that an equivalent dependence of shear modulus on configurational enthalpy arises via a thermal softening path, we have established that this dependence of shear modulus on configurational enthalpy is essentially a unique functional relation.

Furthermore, since there are two independent processes that result in the same dependence of shear modulus on configurational enthalpy it is evident that it does not matter how a particular configurational state is reached. A final state may be reached by deformation, thermal excitation, radiation, or any other means of changing the mean energy of the system. All that is relevant for predicting the properties of the material is the amount of energy that has been stored in it. Furthermore, since there is a unique functional relation between the configurational energy of the system and the isoconfigurational shear modulus, we can predict the properties of the material by simply measuring the isoconfigurational shear modulus.

5.6 References

[1] F. Spaepen, Acta Metall. 25, 407 (1977).

[2] F Spaepen, and D Turnbull, Scripta Metall. 8, 563 (1974).

[3] P A Duine, J Sietsma, and A van den Beukel, Acta metall. mater. 40, 743 (1992).

[4] P S Steif, F Spaepen, and J W Hutchinson, Acta Metall. 30, 447 (1982).

[5] Bas van Aken, P de Hey, and Jilt Sietsma, Mat. Sci. Eng. A 278, (2000) 247.

[6] P de Hey, J Sietsma, and A van den Beukel, Acta Mater. 46, 5873 (1998).

[7] A. S. Argon, Acta Metall. 27, 47 (1979).

[8] A S Argon, and L T Shi, Acta Metall. 31, 499 (1983).

[9] J Megusar, A S Argon, and N J Grant, Mat. Sci. and Eng. 38, 63 (1979).

[10] V A Khonik, Phys. Stat. Sol. (a) 177, 173 (2000).

[11] F H Stillinger, Science 267, 1935 (1995).

[12] W. L. Johnson, and K. Samwer, Phys Rev. Lett. 95, 195501 (2005).

[13] M.L. Lind, G. Duan, and W.L. Johnson, Phys. Rev. Lett. 97, 015501 (2006).

[14] M.D. Demetriou, J.S. Harmon, M. Tao, G. Duan, K. Samwer, and W.L. Johnson, PRL 97, 065502 (2006).

[15] G. Duan, M.L. Lind, M.D. Demetriou, W.L. Johnson, W.A. Goddard III, T Cagin, and K. Samwer, Appl. Phys. Lett. (In press).

[16] K. Ito, C.T. Moynihan, and C.A. Angell, Nature 398, (1999) 492.

[17] L.-M. Martinez, and C.A. Angell, Nature 410, 663 (2001).

[18] L.-M. Wang, V. Velikov, and C.A. Angell, J. Chem. Phys. 117, 10184 (2002).

[19] J. S. Harmon, M. D. Demetriou, and W. L. Johnson, Appl. Phys. Lett. 90, 171923 (2007).

[20] J Schroers, and W L Johnson, Appl. Phys. Lett. 84, 255506 (2004).

[21] M D Demetriou, J S Harmon, M Tao, G Duan, K Samwer, and W L Johnson, Phys. Rev. Lett. 97, 065502 (2006).

[22] N Nishiyama, and A Inoue, Mat. Tran. JIM 37, 1531 (1996).

[23] J Lu, Ph.D. Thesis. Pasadena: California Institute of Technology (2002).

[24] E. Schreiber, O. Anderson, and N. Soga, Elastic Constants and their Measurement, New York: McGraw-Hill (1973).

[25] P. Tuinstra, R. A. Duine, J. Sietsma, and A. van den Buekel, Acta Metall. Mater. 43, 2815 (1995).

[26] M L Lind, unpublished.

[27] N. Nishiyama, A. Inoue, and J. Z. Jiang, Appl. Phys. Lett. 78, 1985 (2001).